The Ultrastructure of Local Lesions Induced by Potato Virus X: a Sequence of Cytological Events in the Course of Infection

A. V. Allison and T. A. Shalla

Department of Plant Pathology, University of California, Davis 95616. We thank Margie Allison for the drawings in Figs. 8 and 16.

Accepted for publication 20 December 1973.

ABSTRACT

Expanding necrotic lesions induced by potato virus X (PVX) in leaves of *Gomphrena globosa* were studied by fluorescence and electron microscopy. When lesions and their marginal tissues were sampled radially, it was possible to determine the sequence in which some infection products were formed. Amorphous inclusion body components, typical of those induced by PVX in systemic host plants, were observed only in cells close to the necrotic center of the lesions, while virus particles were found at greater radial distances in the cytoplasm and plasmodesmata. Abnormal deposits of callose were distributed, primarily in pit areas, to greater radial distances than either inclusion body components or virus particles in the cytoplasm. Complex plasmodesmata and membrane-bound bundles of virus particles embedded in callose outside the protoplast, paralleled the distribution of heavy callose deposits. The extraprotoplasmic sacs of virus in adjacent cells were often connected by plasmodesmata. Since inclusion body components were formed relatively late in the course of infection, it is concluded that they do not function as virus factories. It is proposed that callose deposition and exclusion of virus particles from the protoplast may constitute a mechanism for limiting the spread of virus in hypersensitive tissue.

Phytopathology 64:784-793.

The ultrastructure of plants systemically infected with potato virus X (PVX) has been described extensively (2, 7, 12, 17). Infected cells contain proteinaceous sheets, either smooth or studded with ribosomelike particles, which occur in laminated bundles or scrolls and are prominent structural components of amorphous inclusion bodies. Whether or not these inclusion body components play any biological role in the infection process is not known. It has been proposed that they may be sites of virus synthesis (7). However, Shalla and Petersen (11) have shown that their formation was delayed in isolated leaf protoplasts synchronously infected with PVX. Their appearance long after that of viral antigen and subsequent to the formation of PVX particles themselves, was given as evidence against their involvement in structural protein synthesis.

One means of determining the sequence of events during plant virus replication is to examine the progressive stages of infection occurring in cells at the margins of visible, spreading infection centers (i.e., local lesions) on manually inoculated leaves. A local lesion represents a focus of infection from which virus particles move radially, colonize new cells, replicate, and move again. Therefore, examination of a local lesion along its radius should reveal the sequence of events in the infection cycle; the earliest events being in cells most peripheral, and the later ones occurring in cells toward the center of the lesion. The purpose of this study was to determine the order in which inclusion body components and virus particles were formed by examining cells at the margin of PVX-induced lesions on leaves of *Gomphrena globosa* L., a more natural virus-host relationship than is

represented by infection of isolated protoplasts. During these studies, additional ultrastructural changes were observed which may explain how the movement of virus through hypersensitive tissues is ultimately restricted.

MATERIALS AND METHODS.—*Host and viral isolate.*—Seedlings of *Gomphrena globosa* L. at the eight-leaf stage were placed in growth chambers for 72 h prior to inoculation. The chambers were set continuously at 20 C and had both cool-white fluorescent and incandescent light. *G. globosa* was chosen because it responds to PVX infection with expanding necrotic lesions.

The isolate of PVX was a mottle strain initially obtained from a naturally infected potato plant in Montana. For use as inoculum, virus was purified by a modification of the method of Shepard and Secor (13). Leaves were manually inoculated with virus at a concn of 1 mg/ml which resulted in the formation of 5-15 lesions/leaf.

Infectivity and lesion size.—To establish that an increase in lesion size was accompanied by virus multiplication, leaf disks 5 mm in diam and containing one local lesion each were cut from *G. globosa* leaves at 96 and 168 h after inoculation with PVX. Samples of five leaf disks were stored at −20 C, then thawed and ground with 10 drops of 0.05 M borate buffer (pH 8.2) in a ground-glass homogenizer. The respective samples were assayed on four pairs of opposite half-leaves of *Chenopodium amaranticolor* Coste & Reyn. The resulting number of lesions was counted after 9 days.

The diam of 10 local lesions on three different plants was measured twice daily between 86 and 190 h after inoculation and once daily thereafter up to about 240 h. Measurements were made with an ocular micrometer in a dissecting microscope. A line of India ink marked on the leaves showed that there was no appreciable increase in leaf size during the time of lesion growth.

Electron microscopy.—Approximately 100 h after inoculation, lesions were excised, fixed in 3% glutaraldehyde, postfixed in 2% osmium tetroxide, dehydrated in acetone, and embedded in a low-viscosity epoxy resin (16). Pieces of healthy leaves were similarly prepared for controls. Tissue sections were cut with a diamond knife on a Porter-Blum microtome. For routine microscopy they were picked up on uncoated 300-mesh grids, whereas, serial sections were retrieved on collodion membranes supported by lucite rings, and then transferred to EFFA bar grids (19). Sections were stained with uranyl acetate followed by lead citrate and examined with an RCA EMU 3H or an AEI EM6-B electron microscope.

Fluorescence microscopy.—For histochemical identification of callose, leaves of *G. globosa* bearing local lesions were killed and fixed in a crushed dry-ice/ethanol-acetic acid system [95% ethanol and glacial acetic acid (3:1, v/v)]. Noninoculated leaves were similarly prepared for controls. The tissues were embedded in a gelatin-glycerol medium (30 ml water, 1.5 ml glycerol, 7 gm gelatin), frozen on dry ice, and sectioned to about 100 μm on a cryostat. Sections were stained with 0.1% aniline blue fluorochrome (4). Alternate unstained sections were prepared as controls. Observations were made with a Zeiss microscope equipped with a high

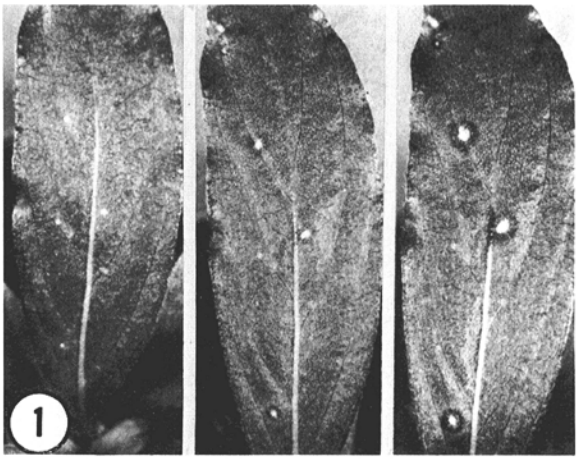

Fig. 1. Local lesions on *Gomphrena globosa* at 96 (left), 150 (center), and 240 (right) h after inoculation with potato virus X.

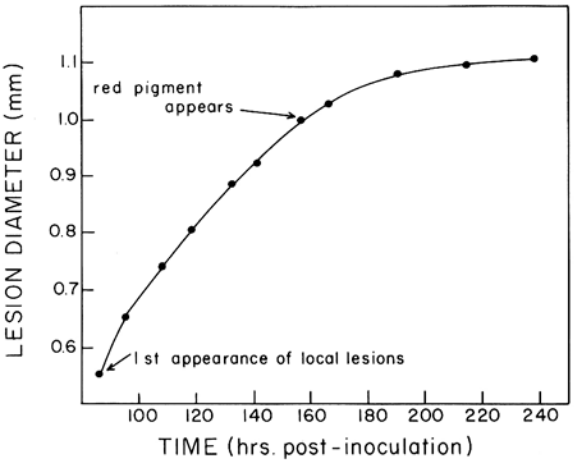

Fig. 2. Diam of local lesions on *Gomphrena globosa* leaves at different times after inoculation with potato virus X. Diam is the average of 10 local lesions at each sampling time.

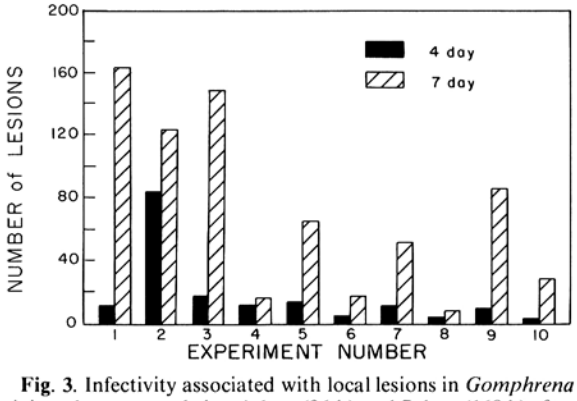

Fig. 3. Infectivity associated with local lesions in *Gomphrena globosa* leaves sampled at 4 days (96 h) and 7 days (168 h) after inoculation with potato virus X. Infectivity is the total number of local lesions produced on four half-leaves of *Chenopodium amaranticolor* by a sample containing five local lesions per experiment from *Gomphrena globosa*.

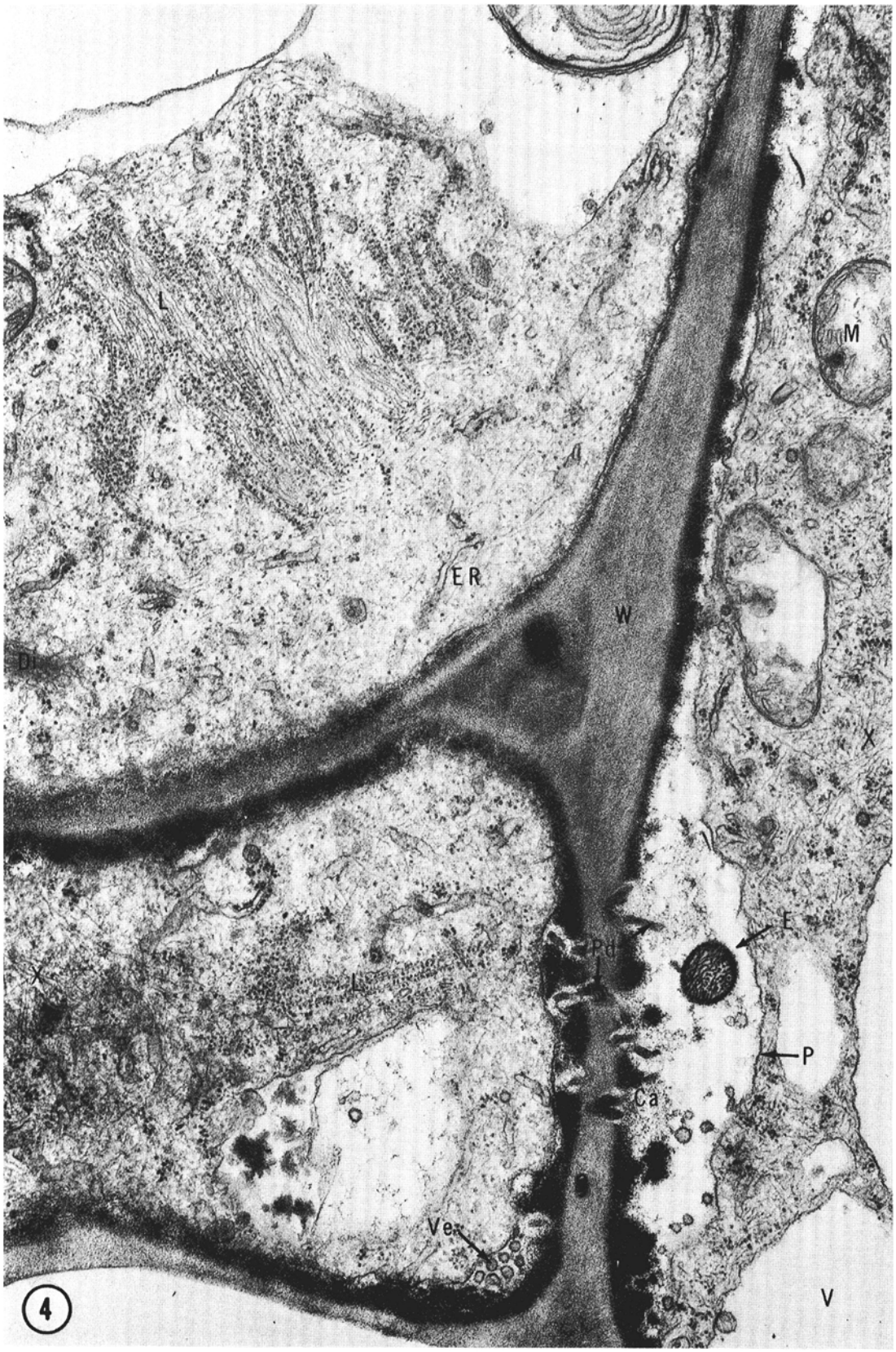

Fig. 4. Portions of three cells from the zone immediately adjacent to necrotic cells of a potato virus X (PVX) lesion sampled at 96 h post inoculation. Callose (Ca) is interposed between the plasmalemma (P) and the primary cell wall (W) which is penetrated by complex plasmodesmata (Pd). An extraprotoplasmic sac of virus (E) is embedded in the callose. PVX particles (X) are found scattered in the cytoplasm, which also contains laminate inclusion components (L). ER, endoplasmic reticulum; M, mitochondrion; V, vacuole; Ve, vesicles. × 33,600.

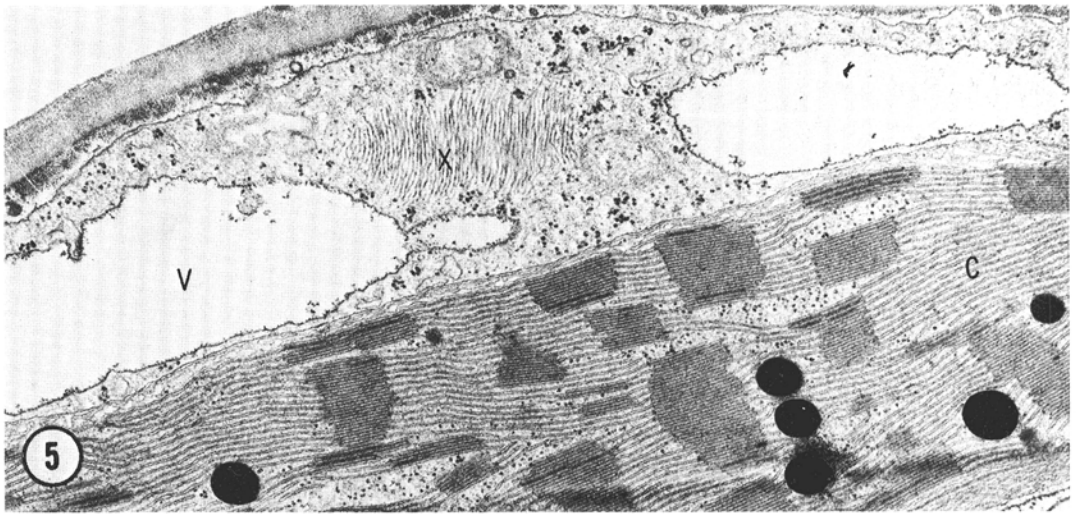

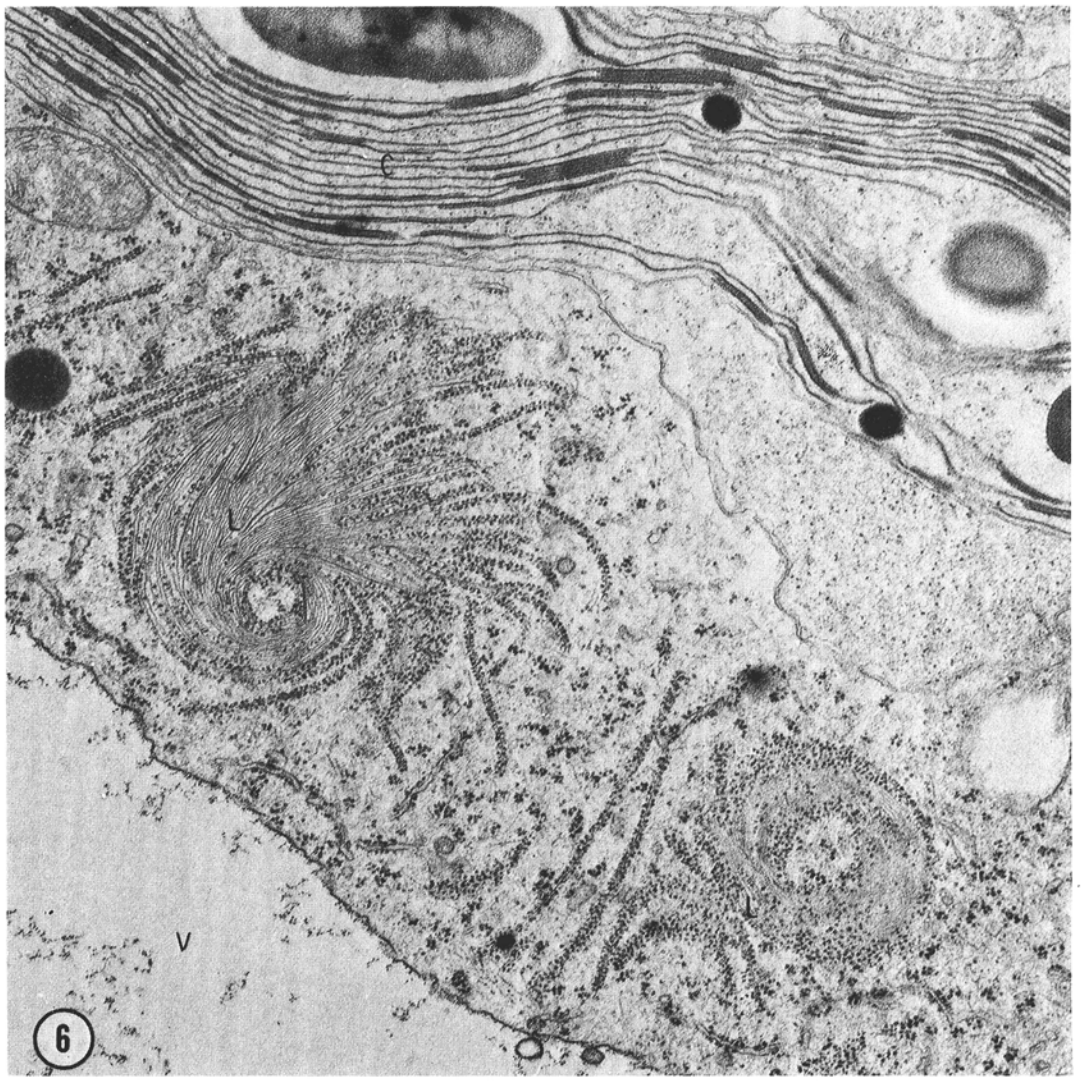

Fig. 5-6. Potato virus X in leaf of *Gomphrena globosa*. **5)** Part of a mesophyll cell, 10 cells removed from the necrotic margin of a lesion. A typical small aggregate of potato virus X particles (X) is in the cytoplasm. V, vacuole; C, chloroplast. × 26,880. **6)** Laminate inclusion components (L) in scrolls of smooth and beaded sheets in a cell adjacent to the necrotic part of a lesion. Chloroplast (C) has begun to disintegrate. V, vacuole, × 20,760.

pressure mercury lamp (HBO 200 W). Two BG12 exciter filters with a maximum transmission of 420 nm in conjunction with an OG 5 barrier filter provided blue-light illumination. For comparison, ultraviolet (UV) illumination provided by a BG12 (366 nm max.) exciter filter with barrier filters BG23 plus GG4 was used for more specific identification of callose (4).

RESULTS.—*Macroscopic observations of local lesion development.*—Lesions first became visible to the unaided eye at 84-96 h after inoculation (Fig. 1, left). The necrotic lesion gradually enlarged in diam, growing most rapidly until about 200 h when the rate of growth declined (Fig. 1, right, Fig. 2). At about 150 h, a reddish halo appeared in the tissue adjacent to the necrotic center (Fig. 1, center, right). Lesion growth was accompanied by an increase in infective material. Homogenates prepared from 168 h (7 day) local lesions were always more infective than ones from 96 h (4 day) lesions when assayed on opposite half-leaves of *C. amaranticolor* (Fig. 3). Since there was rapid expansion of lesions and active virus multiplication at 96 h after inoculation, lesions were sampled at that time for microscopic study.

Ultrastructure of expanding lesions.—The necrotic center of lesions was composed of cells with disorganized contents. Fragments of chloroplasts, aggregates of ribosomes, starch grains, and virus particles were recognizable. The remnant of the protoplast was plasmolyzed, and the intercellular cytoplasmic connections were often severed.

The region of living, but moribund, cells immediately adjacent to the necrotic center contained cells with cytological features indicating unusual metabolic activity: wall thickenings, occluded plasmodesmata, numerous dictysomes, inflated endoplasmic reticulum, virus particles, and laminate inclusion body components (Fig. 4). The area of greatest change was immediately adjacent to the necrotic cells and graded centrifically into normal tissue.

Virus particles were both scattered at random in the cytoplasm and in small aggregates (Fig. 5) for up to ten

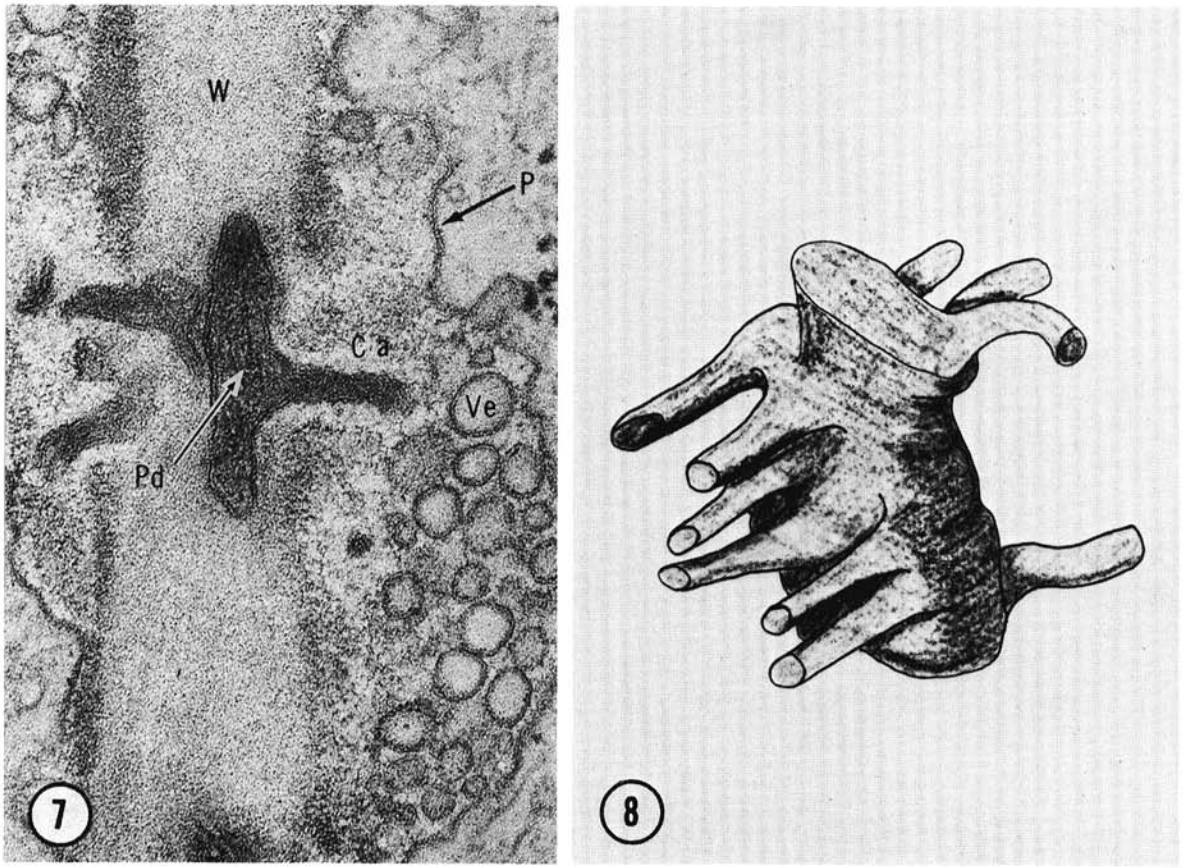

Fig. 7-8. Complex plasmodesmata produced in tissues of *Gomphrena globosa* during infection by potato virus X. **7)** One section from a series through a complex plasmodesma (Pd) several cells distal to the necrotic zone. The plasmalemma (P) is invaginated, and the plasmodesmal canal distended. The callose (Ca) which is interposed between the primary cell wall (W) and the plasmalemma contains single membrane-bound vesicles (Ve). Although in this section the plasmodesma arms appear to be isolated, serial sections revealed that most of them were continuous with the cytoplasm of both cells. × 86,700. **8)** Three-dimensional interpretation of complex plasmodesma constructed from serial sections. The section shown in Fig. 7 was one of those used to reconstruct this model and shows only a part of the large central cavity and its complex branching. The plasmodesmal canals are distended beyond where they normally end at the edge of the primary wall.

cells from the margin of necrosis. Amorphous inclusion body components were commonly observed in cells adjacent to necrotic centers, but never more than the third cell removed from the margin of necrosis (Fig. 4, 6). These consisted of smooth and beaded sheets often formed into scrolls (Fig. 6), identical to those described in systemic hosts of PVX (12).

Plasmodesmata often were branched with the plasmodesmal canals extending away from the primary cell wall. Although canals often appeared to terminate in a matrix populated with vesicles between the primary cell wall and the plasmalemma (Fig. 7), examination of serial sections revealed that most of them terminated in the cytoplasm. A study of serial sections also revealed that rather than being a simple or sparsely branched tube through the wall, such plasmodesmata were highly branched and complex. The arms were extensions of a central cavity in the cell wall (Fig. 7, 8). Such complex branching was also observed in noninoculated leaves, but the extension of the arms was only seen in relation to lesion development, the greatest extension proximal to the necrotic center and diminishing distally. Figure 8 shows a diagrammatic representation of such a complex plasmodesmata which was constructed from a series of eight serial sections, one of which is shown in Fig. 7.

The central cavity of such complex plasmodesmata often contained virus particles (Fig. 9, 10). Both longitudinal and cross-sectional views of the virus particles could be found in the same cavity (Fig. 10). Desmotubules, usually evident in plasmodesmata of healthy tissue, were occasionally also seen in plasmodesmata that contained virus particles (Fig. 10).

Deposits of electron-transparent material occurred along large areas of the cell wall (Fig. 4, 11), particularly in proximity to plasmodesmata (Fig. 4, 7, 11, 13, 14). These deposits were heaviest near the necrotic zone and diminished radially for about 30 cells distant from the margin of necrosis. When paradermal sections of lesions were stained with aniline blue and examined with the fluorescence microscope, large deposits of callose were demonstrated in association with cell walls surrounding the necrotic zone (Fig. 12). Also numerous small deposits

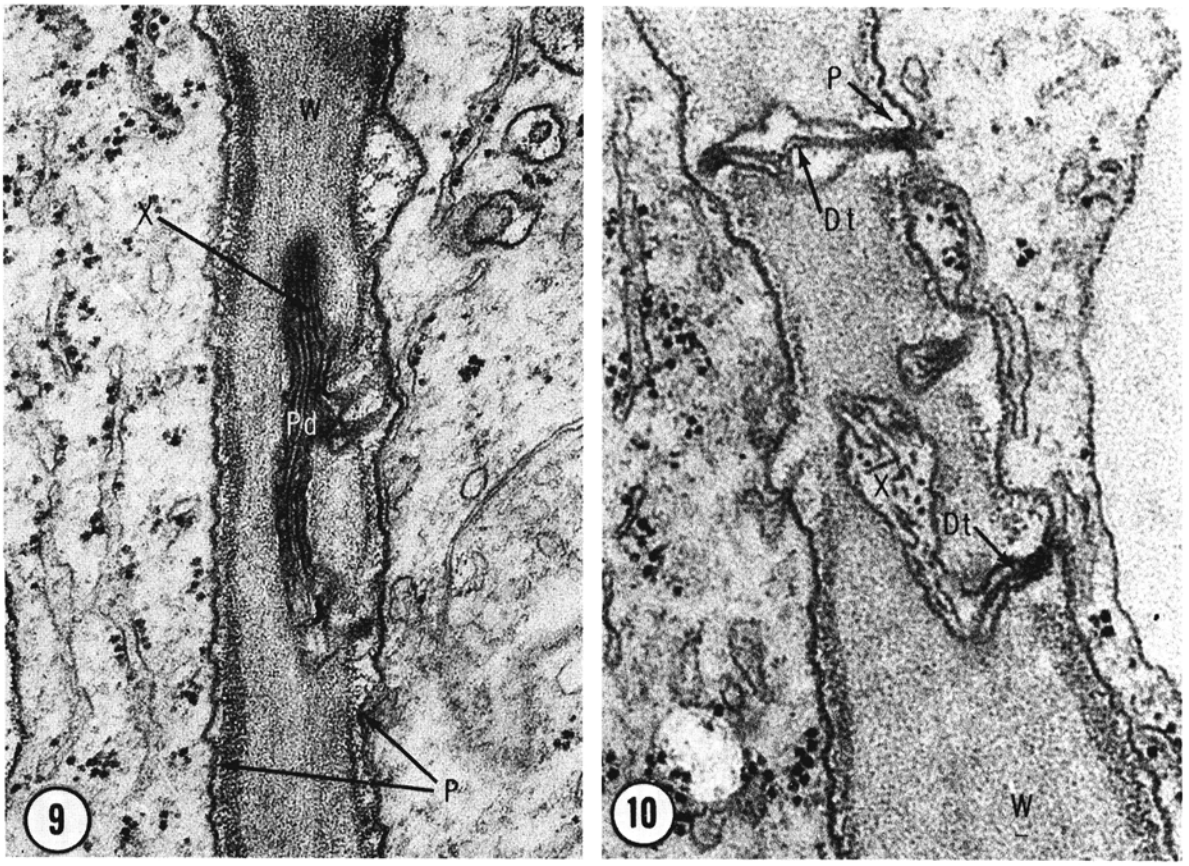

Fig. 9-10. Cytology of potato virus X infection of a *Gomphrena globosa* leaf. **9)** Section through a portion of a complex plasmodesmata (Pd) containing virus particles (X). W, wall; P, plasmalemma. × 43,452. **10)** Plasmodesmata between mesophyll cells several cells from the necrotic zone. In the upper plasmodesma, the neck of the plasmodesma is distended slightly beyond the normal wall (W), but the plasmalemma (P) is continuous with the lining of the plasmodesmal canal and cavity. The desmotuble (Dt) appears to traverse the entire canal. In the lower plasmodesma, virus particles (X) appear in longitudinal and cross-section, and the desmotubule (Dt) is evident in the right hand terminus. × 56,304.

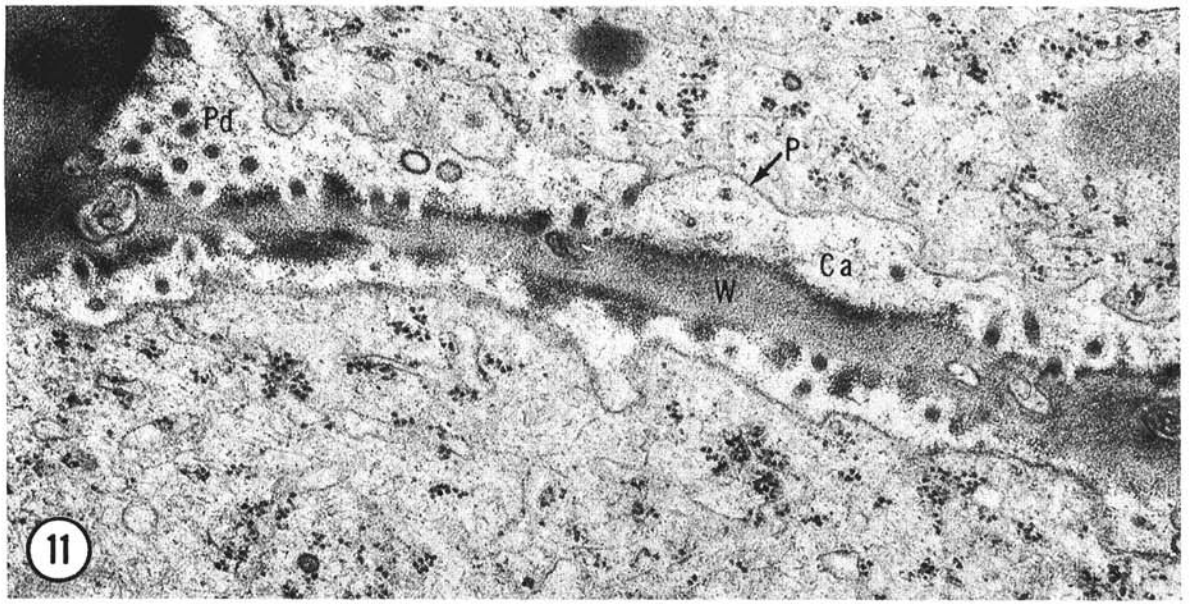

Fig. 11. Extensive callose (Ca) deposition along the primary walls (W) between two mesophyll cells close to the necrotic zone. Compare with the fluorescence micrograph in Fig. 12. Note the plasmodesmata (Pd) seen in cross-section. P, plasmalemma. ×28,560.

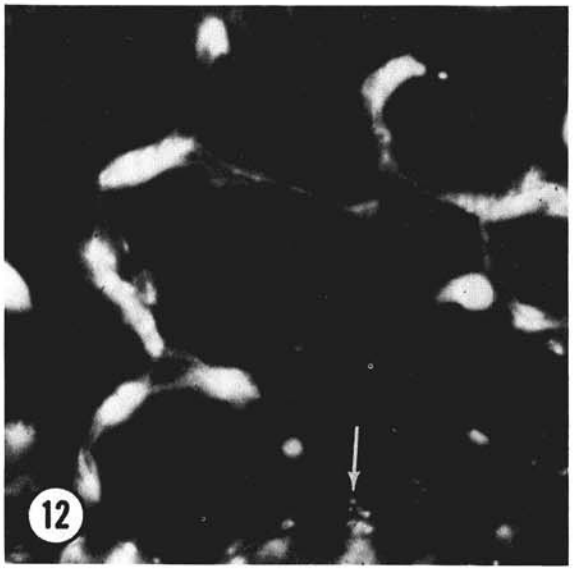

Fig. 12. Fluorescence micrograph of a paradermal section through a region peripheral to the necrotic zone of a local lesion. The section has been stained with aniline-blue to demonstrate callose. The light areas represent callose (compare with Fig. 11). Arrow points to a more limited deposit of callose in a pit area. × 2,200.

of callose occurred in the pit areas (Fig. 12, arrow). The aniline blue-stained callose observed by fluorescence microscopy had the same distribution in individual cells and with respect to the lesion as a whole as the material of low electron density observed with the electron microscope. Therefore, the latter probably depicts deposits of callose mainly around complex plasmodesmata.

Membrane-bound aggregates of virus in extraprotoplasmic space occurred within up to about 10 cells outside the necrotic zone (Fig. 13-16). While most plasmodesmal canals were continuous with the cytoplasm, some terminated in virus-filled sacs embedded in the callose matrix deposited between the plasmalemma and the primary cell wall. From a critical study of serial sections, these sacs were shown to be closed structures completely excluded from the protoplast. These extraprotoplasmic sacs of virus were found on both the distal and proximal sides of cell walls relative to the center of the lesion. Occasionally they were seen on both sides connected with each other by a plasmodesmal canal (Fig. 15). A diagrammatic representation showing the essential details of such a sac based on the information obtained from a study of 10 serial sections is shown in Fig. 16.

DISCUSSION.—PVX-induced lesions provided a valid system for studying the order in which virus particles and inclusion body components were formed. The increase in infectivity associated with local lesion

Fig. 13-16. Extraprotoplasmic sacs of virus (E) in pit areas of cells near the necrotic zone. **13)** Cross-section through sac of virus (E) embedded in callose (Ca). × 41,961. **14)** Longitudinal section through sac and connecting with a complex plasmodesmata (Pd). × 41,961. **15)** Two extraprotoplasmic sacs of virus connected by a plasmodesmal canal (arrow). Virus particles in the sacs can be seen in both longitudinal and cross-sectional view. × 76,538. **16)** Idealized model demonstrating the relationship of the sac of virus to the cell wall (W) and callose deposit (Ca). The model was reconstructed from a study of serial sections. ER, endoplasmic reticulum; M, mit :hondrion; P, plasmalemma; Ve, vesicle; W, cell wall.

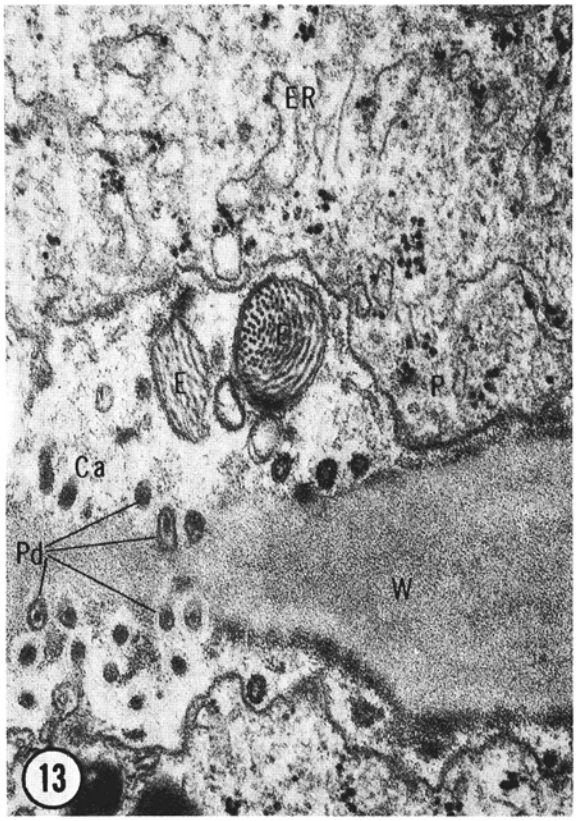
ER
E
P
Ca
Pd
W
13

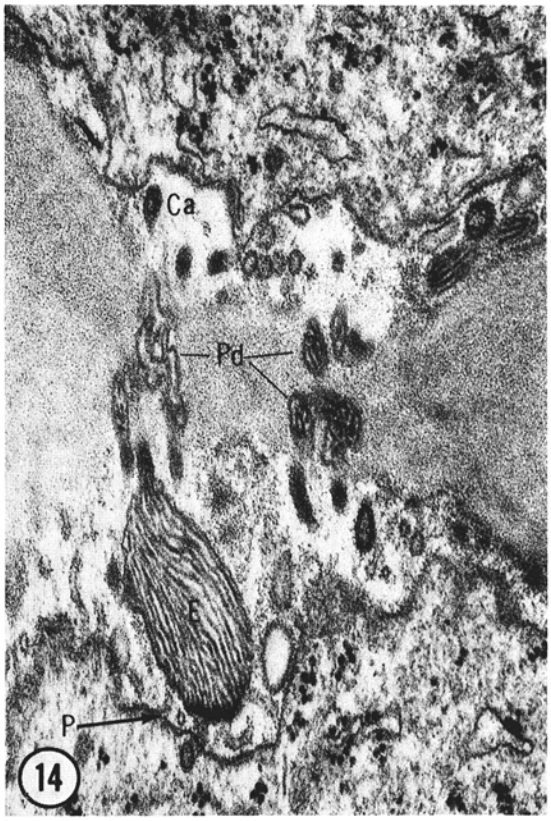
Ca
Pd
E
P
14

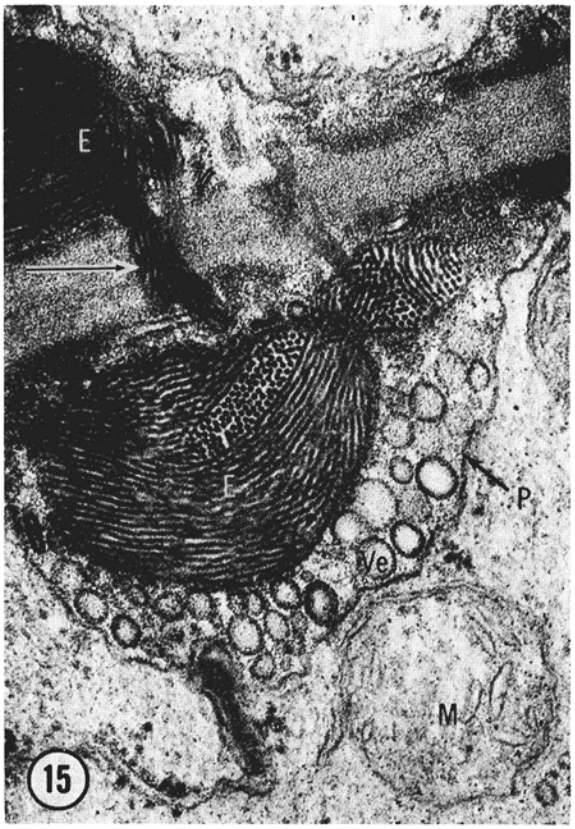
E
F
P
Ve
M
15

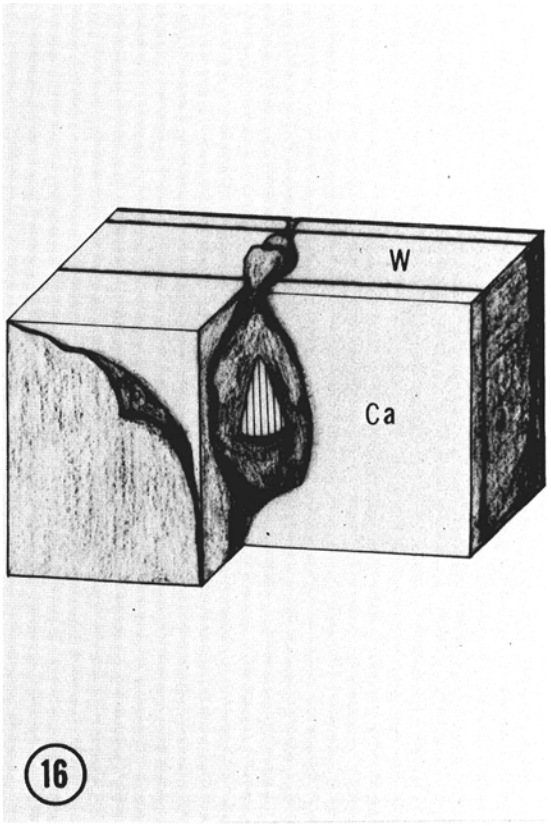
W
Ca
16

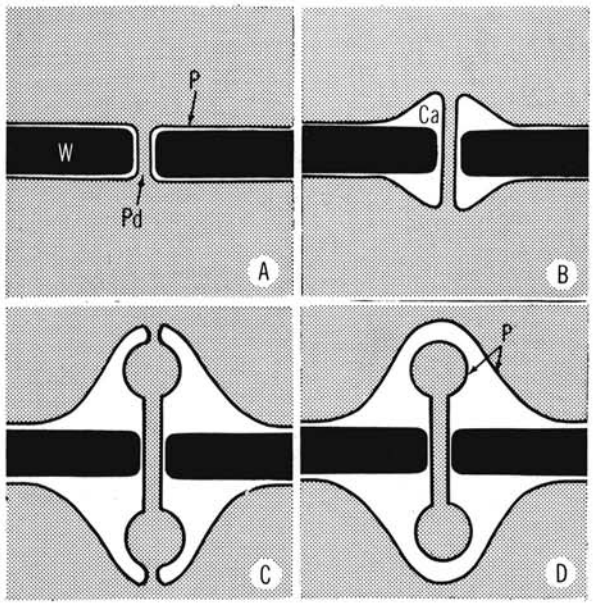

Fig. 17-(A to D). Simplified diagrams showing the probable means by which sacs of cytoplasmic material (shaded regions) are sealed off from the protoplast by callose deposition in *Gomphrena globosa* leaf tissue during infection by potato virus X. **A)** normal plasmodesma (Pd). **B-D)** progressive deposition of callose (Ca). W, primary cell wall; P, plasmalemma.

expansion, and the occurrence of virus particles in plasmodesmata were consistent with the belief that an increase in lesion size was the result of a continuous radial invasion of cells and multiplication of virus therein. Thus, those cells located some distance from the necrotic zone would be in relatively early stages of the infection cycle, whereas those close to the zone of necrosis would be at more advanced stages. Since virus particles were invariably found further from the necrotic region than inclusion body components, it is concluded that the inclusion components were formed later in the process of infection than the virus itself. This agrees with the findings of Shalla and Petersen (11) that the inclusion body components were formed late in the infection cycle relative to the viral antigens detected in isolated protoplasts inoculated with PVX. Therefore, they are probably not the sites of virus protein synthesis, despite the ribosome-like appearance of the beads. Their function remains unknown.

Although virus particles and inclusion components were common in cells marginal to the necrotic zone, the most dramatic and widespread modifications involved the cell wall and associated structures. Deposition of callose was the most common structural change. Minor deposits in pit areas distal to the necrotic zone represented the earliest stages of lesion formation. Callose deposition increased progressively, becoming inordinately heavy around plasmodesmata and along large areas of the walls of cells close to the necrotic zone. The protrusion of the arms of the plasmodesmata was interpreted to be a consequence of callose deposition between the plasmalemma and the primary cell wall. The most severely distorted plasmodesmata were closest to the necrotic center where callose deposition was heaviest. Similarly, the formation of the extraprotoplasmic sacs of virus was probably due to excessive callose deposition. Figure 17 illustrates diagrammatically one way in which sacs of cytoplasmic material (including virus aggregates) could have become excluded from the protoplast through progressive deposition of callose in the vicinity, in this case, of a simple plasmodesma. This scheme is supported by electron micrographs which depict step B (see Fig. 10 at P) and step D (see Fig. 15), but step C has not been observed. Such a mechanism could, conceivably, restrict the cell-to-cell movement of virus.

Several theories on mechanisms for localizing a virus infection by physically restricting its movement have been advanced. Simmons et al. (14) suggested that virus movement is limited by collapse and death of cells in advance of the virus, thus rendering further movement and multiplication of virus impossible. Alternatively, since intercellular virus movement is believed to take place via the plasmodesmata (3, 10), either mechanical blockage of the plasmodesmata by callose (5, 20) or severance of the plasmodesmata (15) could block cell-to-cell movement of virus. Since the deposits of callose in pit areas and modification of the plasmodesmata observed in this study were found at greater radial distances from the necrotic zone than virus particles in the plasmodesmata or cytoplasm, it seems reasonable that callose deposition and the resulting plasmodesmatal deformation could function ultimately in restricting virus movement. It should be noted that PVX is not known to induce callose deposition in systemic hosts, such as tobacco and *Datura stramonium* L.

Conditions which are known to inhibit callose deposition, such as holding plants in the dark (18), have also been reported to enhance the movement of viruses in local lesion hosts. Wu and Dimitman (20) utilizing dark treatment plus UV irradiation of inoculated leaves, prevented callose deposition and caused an increase in the size of lesions induced by tobacco mosaic virus in bean leaves. Similarly, detached leaves of *G. globosa* which were incubated in the dark after inoculation with PVX, sustained a limited systemic infection instead of developing local lesions (6).

The presence of extraprotoplasmic sacs of virus particles suggests that virus which normally might have moved from one cell to another had been sealed off by deposits of callose. Whether these structures do, in fact, reflect a manner in which intracellular movement of virus is prevented, or are merely incidental manifestations of callose deposition, is difficult to assess. They occur only rarely in tobacco plants systemically infected with PVX, but excessive callose deposition is also rare. Few reports have been published showing structures resembling these extraprotoplasmic sacs of virus (1, 8, 9). These were all found in hosts systemically infected by viruses of the potato virus Y group. Considering the scarcity of reports about them in the literature, they must rarely occur in systemic hosts in which cell-to-cell movement of virus is comparatively unrestricted.

LITERATURE CITED

1. BARNETT, O. W., G. A. DE ZOETEN, and G. GAARD. 1971. Bearded iris mosaic virus: transmission,

purification, inclusions, and its differentiation from bulbous iris mosaic. Phytopathology 61:926-932.
2. BORGES, M. L. V., and J. F. D. FERREIRA. 1959. Virus na celula vegetal. Observacoes ao microscopia electronico. II. Virus X da batateira. Portugaliae Acta Biol. Serv. A, 6:18-22.
3. ESAU, K., J. CRONSHAW, and L. L. HOEFFERT. 1967. Relation of beet yellows virus to the phloem and to movement in the sieve tube. J. Cell. Biol. 32:71-87.
4. ESCHRICH, W., and H. B. CURRIER. 1964. Identification of callose by its diachrome and fluorochrome reactions. Stain Technol. 39:303-307.
5. HIRUKI, C., and J. C. TU. 1972. Light and electron microscopy of potato virus M lesions and marginal tissue in red kidney bean. Phytopathology 62:77-85.
6. HUGUELET, J. E., and W. J. HOOKER. 1966. Latent infection of Gomphrena globosa by potato virus X. Phytopathology 56:431-437.
7. KOZAR, F. E., and Y. M. SHELUDKO. 1969. Ultrastructure of potato and Datura stramonium plant cells infected with potato virus X. Virology 38:220-229.
8. KRASS, C. J., and R. E. FORD. 1969. Ultrastructure of corn systemically infected with maize dwarf mosaic virus. Phytopathology 59:431-439.
9. LEE, P. E. 1965. Electron microscopy of inclusions associated with wheat streak mosaic virus. J. Ultrastruct. Res. 13:359-366.
10. LIVINGSTON, L. G. 1935. The nature and distribution of plasmodesmata in the tobacco plant. Am. J. Bot. 22:75-87.
11. SHALLA, T. A., and L. J. PETERSEN. 1973. Infection of isolated plant protoplasts with potato virus X. Phytopathology 63:1125-1130.
12. SHALLA, T. A., and J. F. SHEPARD. 1972. The structure and antigenic analysis of amorphous inclusion bodies induced by potato virus X. Virology 49:654-667.
13. SHEPARD, J. F., and G. A. SECOR. 1969. Detection of potato virus X in infected plant tissue by radial and double-diffusion tests in agar. Phytopathology 59:1838-1844.
14. SIMONS, T. J., H. W. ISRAEL, and A. F. ROSS. 1972. Effect of 2,4-dichlorophenoxyacetic acid on tobacco mosaic virus lesions in tobacco and on the fine structure of adjacent cells. Virology 48:502-515.
15. SPENCER, D. F., and W. C. KIMMINS. 1971. Ultrastructure of tobacco mosaic virus lesions and surrounding tissue in Phaseolus vulgaris var. Pinto. Can. J. Bot. 49:417-421.
16. SPURR, A. R. 1969. A low-viscosity epoxy resin embedding medium for electron microscopy. J. Ultrastruct. Res. 26:31-43.
17. STOLS, A. L. H., G. W. HILL-VAN DER MEULEN, and M. K. I. TOEN. 1970. Electron microscopy of Nicotiana glutinosa leaf cells infected with potato virus X. Virology 40:168-170.
18. WEBSTER, D. H., and H. B. CURRIER. 1968. Heat induced callose and lateral movement of assimilates from phloem. Can. J. Bot. 46:1215-1220.
19. WILLIAMS, R. C., and F. KALLMAN. 1955. Interpretations of electron micrographs of single and serial sections. J. Biophys. Biochem. Cytol. 1:301-314.
20. WU, J. H., and J. E. DIMITMAN. 1970. Leaf structure and callose formation as determinants of tobacco mosaic virus movement in bean leaves as revealed by UV irradiation studies. Virology 40:820-827.